Intrinsic Kinetics of the Hydrogen Reduction of Cu_2S

H. Y. SOHN and S. WON

Intrinsic kinetics of the hydrogen reduction of cuprous sulfide (Cu_2S) have been measured. Experiments were carried out in the temperature range 823 to 1023 K using a thermogravimetric analysis method. The reaction was studied in detail using both thin pellets and powder samples. The reaction followed first-order kinetics with respect to the solid reactant concentration as well as the hydrogen concentration. An activation energy of 92.0 kJ/mol (22.0 kcal/g-mole) was obtained for the reaction. Copper produced from the reaction formed filaments which sintered above about 1000 K.

I. INTRODUCTION

WHILE much work has been done on the reduction of metal oxides, that of metal sulfides has not been studied extensively. The direct reduction of sulfides has a very small equilibrium constant, *i.e.*, about 10^{-3} in the temperature range of interest, and, for this reason, has not been useful for extracting metal values from sulfide ores. Because of the growing concern about atmospheric pollution due to the emission of sulfur dioxide from conventional processes for treating sulfide minerals, much attention has been directed in recent years to a number of alternative processes. One of the promising schemes is the hydrogen reduction of metal sulfides in the presence of lime.[1-4] In this scheme, metal sulfides are mixed with lime and reacted with hydrogen. The reaction can in general be described as follows:

$$H_2 + Me_xS = H_2S + xMe \quad [1]$$

$$H_2S + CaO = H_2O + CaS \quad [2]$$

The role of lime is two-fold: (1) it improves the thermodynamics of reaction [1] by removing hydrogen sulfide through reaction [2], and (2) it fixes sulfur as a solid.

Most previous investigations of this scheme have been concerned with determining the effects of experimental conditions on reaction rates and presenting the results as obtained. A systematic analysis of this system is complicated because the overall reaction involves two gas-solid reactions taking place in succession combined with diffusion of several gaseous species. A general approach for modeling such a system has been described in an earlier article.[5] The proper application of the model requires the availability of information on the intrinsic kinetics of reactions [1] and [2] and on the intrapellet diffusion of the gaseous species. With this in mind, we undertook an investigation to determine the intrinsic kinetics of the reaction between chalcocite and hydrogen. The major aim of the work thus was to obtain a global equation for the intrinsic kinetics for such a use rather than to elucidate detailed fundamental reaction mechanisms.

In recent years a substantial amount of research effort[6-14] has been devoted to determining the kinetics of the reactions between metal sulfides and hydrogen. Much of the previous work[7,11,14] has used a dense piece of solid. The results from such work cannot be directly applied to the reaction of fine particles.

In the experimental determination of intrinsic kinetics parameters, it is very important to ensure that the measurements are carried out under such conditions that the overall rate is controlled by chemical kinetics unaffected by diffusional effects.[15,16] The effect of external mass transfer can be minimized by increasing the flow rate of gas past the sample. The effect of interparticle diffusion can be eliminated by using a thin layer of the solid reactant. In this work, therefore, experiments were carried out in the predominantly chemically controlled region using fine powders and pellets having a short diffusion path (*e.g.*, thin disks or thin layers of loose particles).

II. EXPERIMENTAL

Fine powder of N.F. sublimed sulfur supplied by Baker and reagent-grade copper wire supplied by V.W.R. Scientific were used. Cuprous sulfide was prepared by reacting the copper wire and sulfur at 673 K in an evacuated pyrex tube. The excess sulfur in the crushed product was then driven off at 923 K in a flowing stream of helium to obtain essentially pure cuprous sulfide, which was verified by weight loss measurement in hydrogen at 973 K and X-ray diffraction.

The kinetics of reduction were determined by means of the weight loss measurement technique. Experiments were carried out in a conventional thermogravimetric setup, comprising a reaction tube mounted vertically inside a three-zone furnace (Lindberg Model 54357A) maintained at a desired temperature. A schematic diagram of the apparatus is shown in Figure 1. The electrobalance used was a Cahn Model RM-2 or a Cahn Model 1000 unit.

In most experiments, a flat, shallow quartz or platinum tray was used for holding the particles (approximately 40 mg). The platinum tray had holes punched in the bottom to allow flow of the reactant gas, which minimized the diffusional effects. In other experiments, thin pellets were placed vertically in a platinum wire cage in the direction of hydrogen flow. The pellet samples were fabricated by compacting the sulfide particles (−325 +400 mesh) in a cylindrical steel die. The pellets were disk-shaped, 1.27 cm in diameter, ranging in thickness from 0.2 to 0.3 mm. The porosity of the pellet calculated from the apparent density ranged between 0.20 and 0.24. The hydrogen and helium gases used in this work were supplied by Matheson Co.

H. Y. SOHN is Professor in the Department of Metallurgy and Metallurgical Engineering, University of Utah, Salt Lake City, UT 84112-1183. S. WON, a former Graduate Student in the Department of Metallurgy and Metallurgical Engineering, University of Utah, is now Senior Metallurgist with Cyprus Metallurgical Process Corporation, 800 East Pima Mine Road, Tucson, AZ 85725.

Manuscript submitted March 14, 1985.

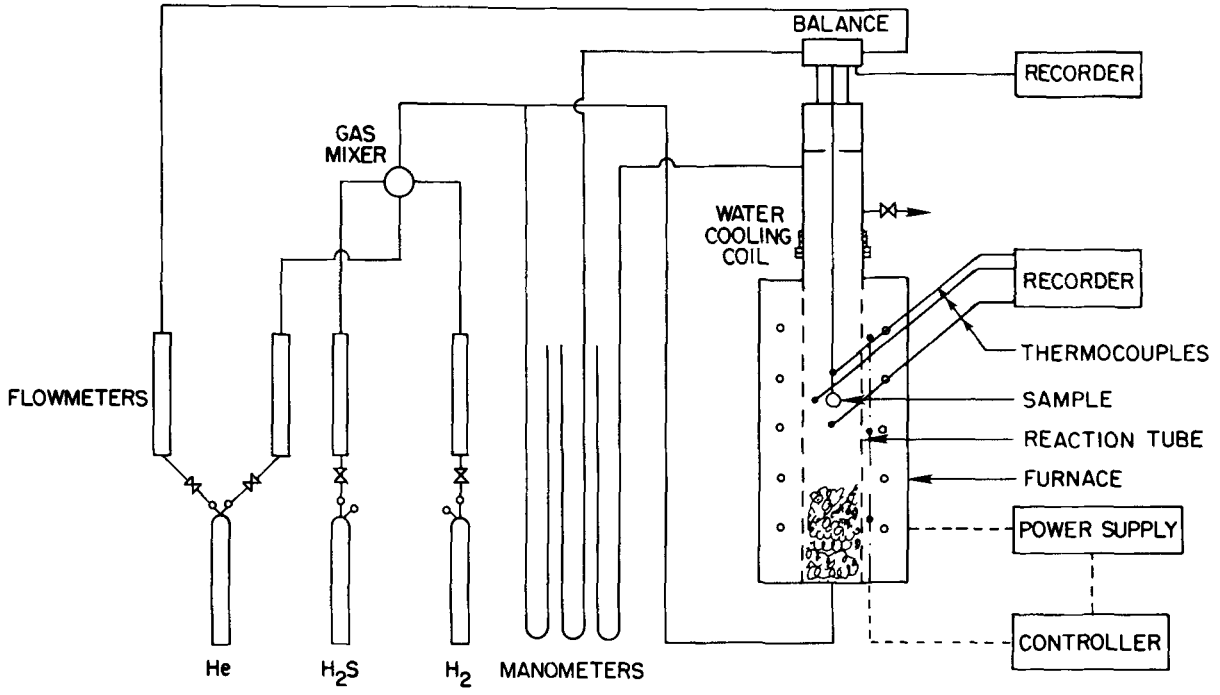

Fig. 1—Schematic diagram of the apparatus.

and were of, respectively, 99.98 and 99.995 pct minimum purity.

The microbalance was first calibrated with standard weights. The solid sample of pellet or particle form was placed in the platinum cage or the quartz tray, which was suspended at the end of a platinum wire. The platinum wire was connected to a gold chain which was in turn attached to one arm of the recording balance. The reaction tube and furnace were then brought into the proper position, and the sample was heated to the desired reaction temperature in a stream of helium. To start the reaction, the gas was switched to hydrogen. The weight change of the solid sample as a function of time was recorded on a recorder. Additional measurements made included the gas flow rate and the reactor temperature around the sample. During the reaction the microbalance was protected from hydrogen sulfide and hot gases by flushing it with helium gas. At the end of a run, the reactant gas was turned off, and the sample was allowed to cool under helium atmosphere. The reaction temperature varied from 823 to 1023 K according to the experimental conditions. Other details of the experimental work can be found in Reference 17.

III. EXPERIMENTAL RESULTS

A. *Characterization of the Sulfide Samples*

The scanning electron micrograph shown in Figure 2 reveals that the unreacted Cu_2S particles (−325 +400 mesh size) had irregular shapes and a highly impervious structure. The examination of the fractured surface taken from a partially reduced Cu_2S pellet at 873 K shown in Figure 3 indicates that the product copper formed filaments on the surface of the reactant sulfide. These filaments grew in bundles having thick bases and thinner ends. The diameters of such filaments ranged between 3 and 8 μm, and the lengths about 1 to 2 mm. The formation of these filaments was observed in the temperature range 823 to 1023 K. At higher temperatures a dense mat of filaments was formed due to the sintering of the product. The filaments were normally curved and thin at low temperature and became shorter and thicker as the temperature increased. The same type of filaments was also found in the powder experiments.

The true specific gravity determined by a Micromeritics 1310 pycnometer was 5.772 for the synthetic sulfide. Nagamori and Ingraham[18] reported the densities of cuprous sulfide ranging from 5.69 to 5.79 depending on the thermal

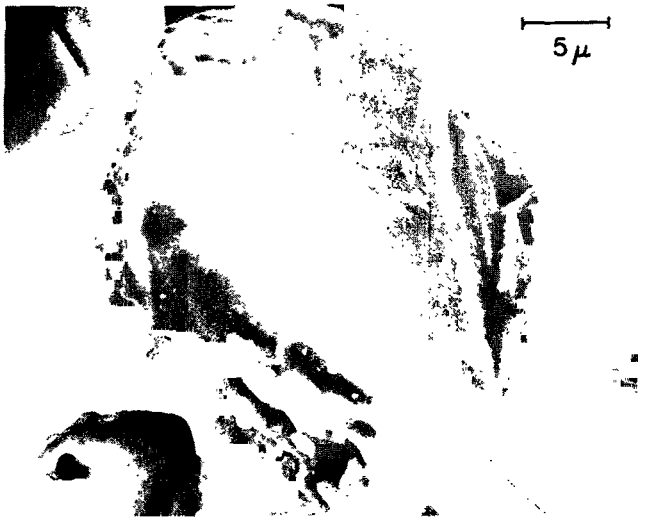

Fig. 2—Scanning electron micrograph showing the impervious surface of the unreacted Cu_2S particle.

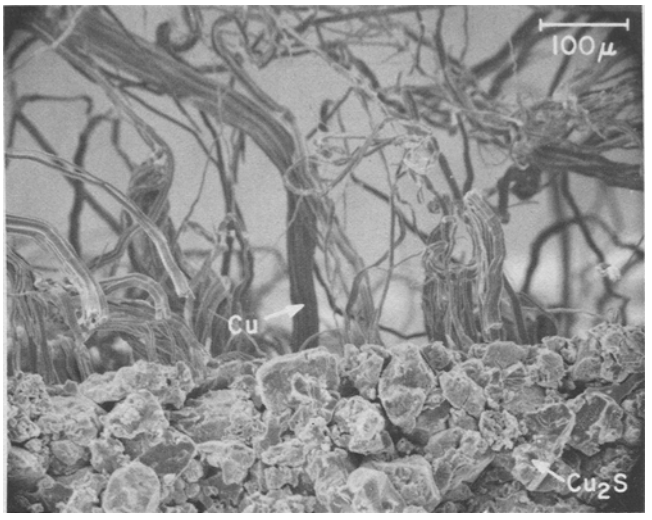

Fig. 3 — Scanning electron micrograph showing the filament formation in a Cu_2S pellet partially reduced at 873 K.

history of the solid. This confirms the absence of micropores in the sulfide particles used in this work. The specific surface area measured by the BET method was 0.763 m^3/g for −325 +400 mesh particle size.

B. *Kinetic Measurement Using Particles*

Since the equilibrium between the gas and the solid phases in this system is attained at very low concentrations of hydrogen sulfide, it can be expected that the effect of external mass transfer would be difficult to eliminate. The critical flow rate beyond which there is no effect of the flow rate on reaction rate was measured at 973 K for a fixed amount of the sample (40 ± 0.5 mg). A hydrogen flow rate of 2.0 dm^3 per minute was determined to be sufficient to reduce the mass transfer resistance to a negligible level by gradually increasing the flow rate until a further increase had no effect on the reaction rate. The subsequent runs were carried out at a constant hydrogen flow rate of 2.0 dm^3 per minute. Interparticle diffusional effects were eliminated by evenly spreading the particles in the sample tray. Sample amounts between 20 to 60 mg resulted in identical conversion rates, indicating that the thickness of the sample layer in this range is small enough not to introduce interparticle diffusional effects. Most subsequent runs were made using sample weights of about 40 mg. The reaction temperature was varied in the range 823 to 1023 K. Typical conversion-time curves for these are given in Figure 4 which shows the effect of temperature on the reaction of −325 +400 mesh size particles in pure hydrogen at 0.86 atm. The reaction at 1023 K did not go to completion because the product filaments tended to sinter and form a dense layer around the unreacted sulfide in the later stage of reduction.

C. *Kinetic Measurements Using Thin Pellets*

Measurements were also carried out using the thin pellet specimens of different thicknesses which ensured that the diffusional effects were small. The pellets were prepared by compacting Cu_2S particles of −325 +400 mesh size.

The critical flow rate of about 10 dm^3 per minute for the absence of mass-transfer effects was determined for pellets of a fixed half thickness of R_p = 0.145 mm ± 10 pct at 973 K. All subsequent experiments were conducted with hydrogen flow rate of 12 dm^3 per minute. The critical flow rate in this case was higher than that for particle samples, because a different apparatus was used.

The effect of sample thickness on the reduction rate of cuprous sulfide is shown for each temperature in Figures 5(a) through (d). As the half thickness R_p was decreased, the

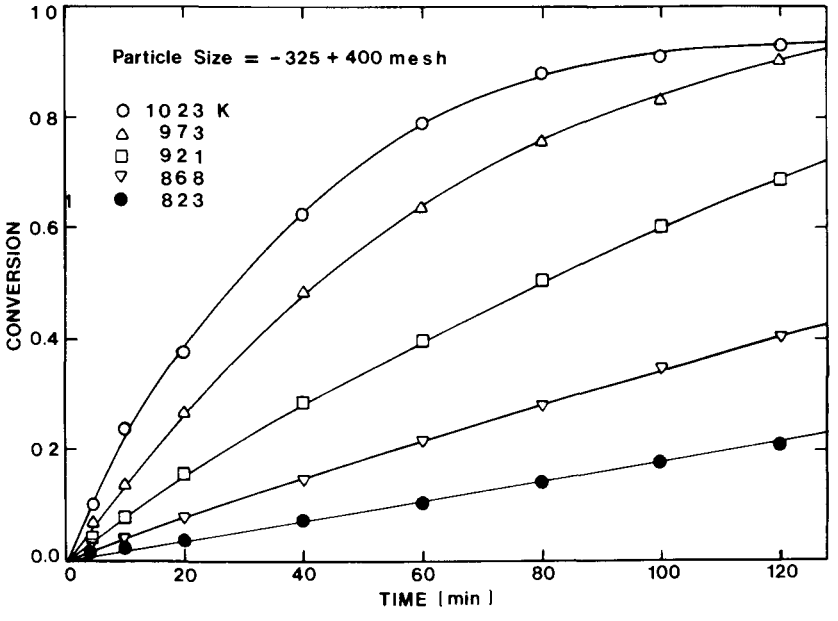

Fig 4 — Effect of temperature on the reaction of Cu_2S particles (−325 +400 mesh; p_{H_2} = 0 86 atm).

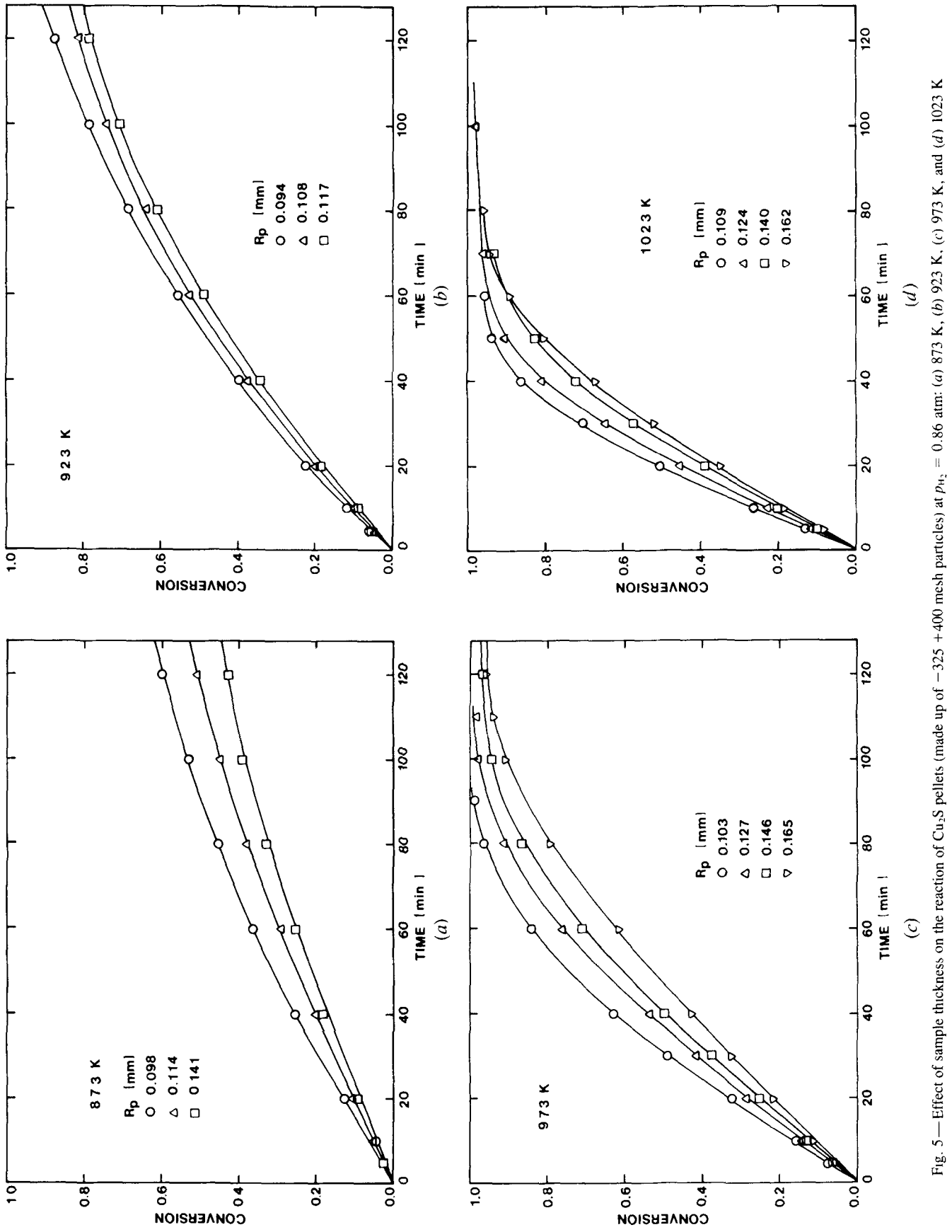

Fig. 5—Effect of sample thickness on the reaction of Cu_2S pellets (made up of −325 +400 mesh particles) at $p_{H_2} = 0.86$ atm: (*a*) 873 K, (*b*) 923 K, (*c*) 973 K, and (*d*) 1023 K

reduction rate increased somewhat in the temperature range 873 to 1023 K. This indicated that the resistance due to pore diffusion was reduced as R_p was decreased. At 1023 K, the conversion of sulfide pellets for various R_p values ceased after about 97 to 98 pct as in the particle experiments due to the formation of a sintered layer around the unreacted sulfide particles.

The concentration of hydrogen was varied by varying the flow rates of hydrogen and helium but maintaining the total flow rate of both gases at 12 dm^3 per minute. The hydrogen concentration ranged from 33 to 100 pct in the gas mixture. The effect of hydrogen concentration on the reduction rate at 923 K is shown in Figure 6.

IV. INTERPRETATION OF RATE DATA

Several investigators[2-4,11-14] have observed the growth of filamentary products (or whiskers) in the reduction of metal sulfides such as those of nickel, cobalt, silver, copper, *etc.* The common feature of the sulfides is that they are known to possess electronic conductivity. According to Wagner,[19] upon heating Cu_2S in hydrogen, sulfide atoms are first removed from the surface, and thus metal/sulfur ratio increases. Then, the metal ions diffuse to the bulk of the metal sulfide, which gradually becomes supersaturated with respect to the metal. Accordingly, nucleation of the metal becomes possible. Once metal nuclei are formed, they are pushed outward from the surface because the stiffness of the sulfur lattice, particularly of the surface layers, restricts the lateral growth, so that a copper filament (or a whisker) grows unidimensionally, as concluded by Hardy[20] for the hydrogen reduction of silver sulfide. In view of the fact that Cu_2S has a relatively high melting point, the filamentary growth would continue from the base in contrast to the growth from such volatile copper salts as CuI and CuCl,[21] in which case filaments may grow from the tip. In the present work, there was no detectable induction period at the beginning of the reaction and no sigmoidal curves, which often characterize the nucleation and growth processes. This can be observed in the experimental results shown in Figures 4 through 6. As described elsewhere,[22,23,24] this phenomenon could be explained by a rapid nucleation rate and one-dimensional filament growth, as shown in Figure 3, taking place in the temperature range of interest. Therefore, the interpretation of the rate data was carried out using the nucleation and growth kinetics. All other rate expressions gave less satisfactory results.

According to a special form of the nucleation and growth kinetics attributed to Erofeev,[25] the conversion, X_B, is related to time, t, by

$$[-\ln(1 - X_B)]^{1/m} = k_b t . \qquad [3]$$

Here, m is a constant and k_b is the apparent rate constant which contains the dependence of the rate on gaseous-reactant concentration and thus can be written as:[26]

$$k_b = b \cdot k \cdot f(C_{H_2}) \qquad [4]$$

where b is the number of moles of solid reacted by one mole of gaseous reactant ($b = 1$ in this work), k is the intrinsic rate constant, C_{H_2} is the hydrogen concentration in the bulk phase, and f designates the dependence of the rate on gaseous-reactant concentration. It is apparent from Eq. [3] that a plot of $\ln[-\ln(1 - X_B)]$ *vs* $\ln t$ should be linear with m as the slope and $m \ln k_b$ as the intercept with the $\ln t = 0$ axis, because C_{H_2} was kept constant.

To study the effect of the hydrogen concentration, the curves which were presented in Figure 6 are replotted in Figure 7 as $\ln[-\ln(1 - X_B)]$ against $\ln t$. The examination of Figure 7 reveals that the data can be fitted by straight lines up to about 90 pct reduction. The values of slopes of 1.01 to 1.10 were obtained by regression analysis, confirming that, as the nucleation and growth kinetics predicted, the nucleation rate was rapid and the growth products were

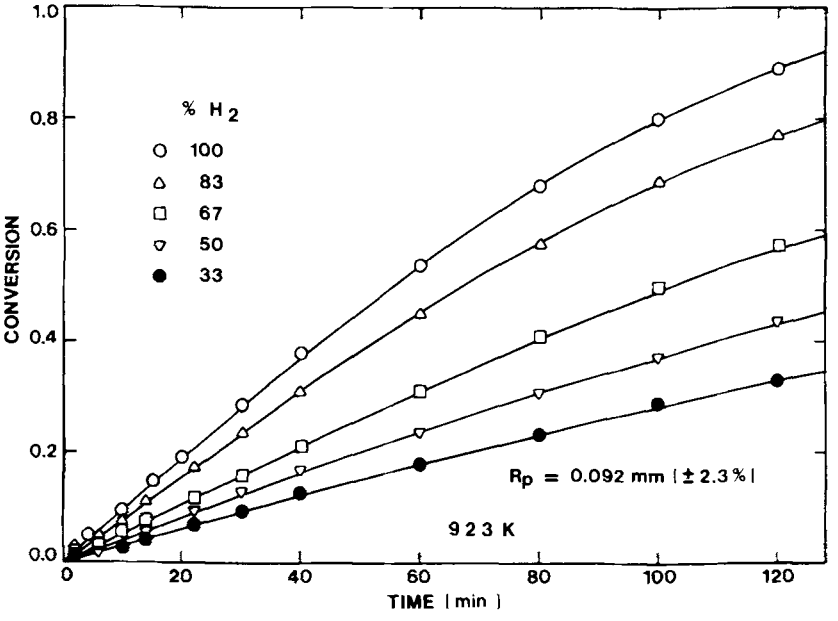

Fig. 6—Effect of hydrogen concentration on the reaction of Cu_2S pellets at 923 K.

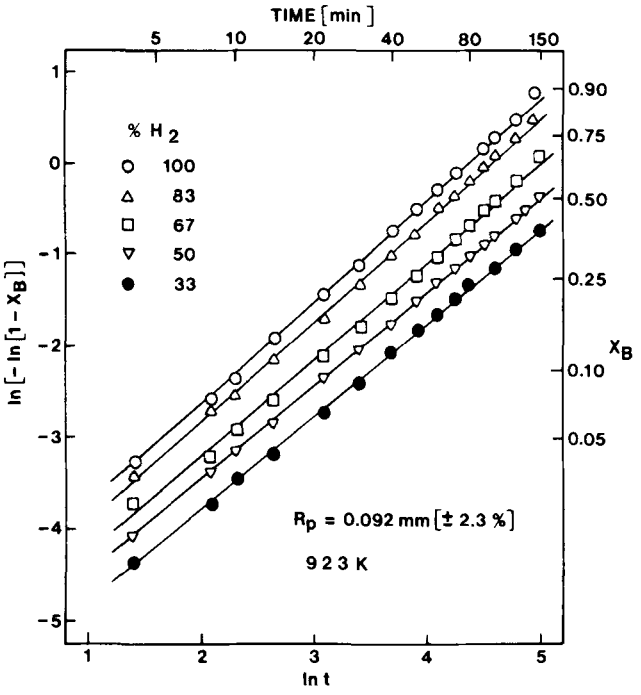

Fig. 7—Plot of $\ln[-\ln(1 - X_B)]$ *vs* $\ln t$ from the result of Fig. 6.

one-dimensional in the range of hydrogen concentration investigated at 923 K. Using this information, the apparent rate constant, k_b, obtained from each intercept is plotted in Figure 8 against the hydrogen concentration according to Eq. [4]. A straight line through the origin is obtained, which is expected for a first-order reaction with respect to the hydrogen concentration in the gaseous mixture of hydrogen and helium and at constant temperature and thus k.

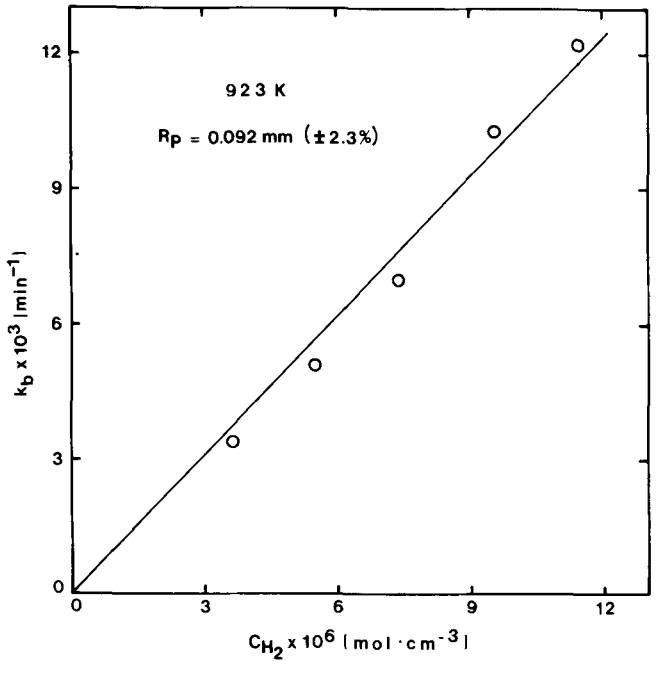

Fig. 8—Dependence of the reduction rate on hydrogen concentration from the results of Fig. 7.

Therefore,

$$f(C_{H_2}) = C_{H_2} \qquad [5]$$

Particle Data: In view of these results, the interpretation of rate data from sulfide particle experiments was made using Eqs. [3] and [4] for the first-order reaction with respect to hydrogen concentration. Figure 9 shows a plot of $\ln[-\ln(1 - X_B)]$ *vs* $\ln t$ obtained from the results of Figure 4. The average value of the slopes was 1.09 (±1.3 pct). Since it would be convenient to use a constant value of m and the values of m are very close to unity, $m = 1$ was used throughout. This is equivalent to a rate expression with a first-order dependence on $(1 - X_B)$. For each temperature, the intrinsic rate constant was calculated from the intercept of Figure 9 using Eq. [4]. The results are shown in Figure 12 as an Arrhenius plot of the rate constants. This figure also shows the results obtained from the pellet experiments, which will be discussed below. The best straight line through the data from the particle experiments may be represented by the equation

$$k = 2.23 \times 10^6 \exp\left(-\frac{E}{RT}\right) (\text{cm}^3 \cdot \text{mol}^{-1} \cdot \text{s}^{-1}) \qquad [6]$$

for −325 +400 mesh size particles, where $E = 92.0$ kJ /mol.

Pellet Data: For a first-order reaction under a small influence of intrapellet diffusion, Sohn and Szekely[27] obtained an approximate relationship between conversion and time. When the reaction is described by the nucleation and growth kinetics, this relationship may be written as

$$[-\ln(1 - x_B)]^{1/m} = (1 - C_1 HR_p^2)k_b t \qquad [7]$$

where C_1 is a constant coefficient whose numerical value depends on the geometry of the system, and R_p is a characteristic dimension of solid. For a slab-like geometry, R_p is

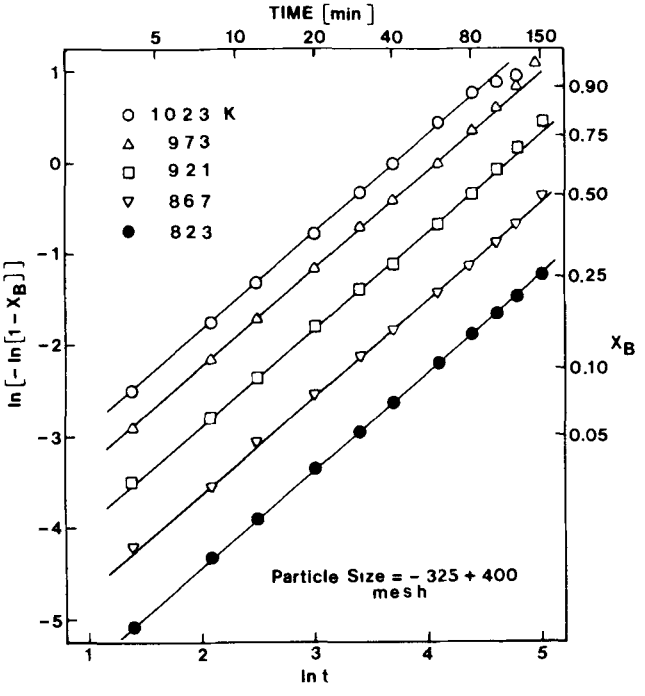

Fig. 9—Plot of $\ln[-\ln(1 - X_B)]$ *vs* $\ln t$ from the results of Fig 4.

the half thickness of the sample. H is a constant independent of R_p containing the rate constant and the effective diffusivity.[15,27]

The constant term multiplying t will be designated by S. Thus,

$$S \equiv k_b - (C_1 H k_b) R_p^2 \quad [8]$$

With this definition, Eq. [7] may be rewritten as

$$[-\ln(1 - X_B)]^{1/m} = St \quad [9]$$

From the experimental results for small but varying disk thicknesses obtained under otherwise fixed conditions, the intrinsic rate constants were obtained at different temperatures through the following procedure:

(1) The conversion-time curves presented in Figures 5(a) through (d) were replotted in Figures 10(a) through (d) as $\ln[-\ln(1 - X_B)]$ against $\ln t$ by using Eq. [9] with $m = 1$. The actual values of m ranged from 1.03 at 897 K to 1.26 at 1023 K. This may be due to the fact that the shape of

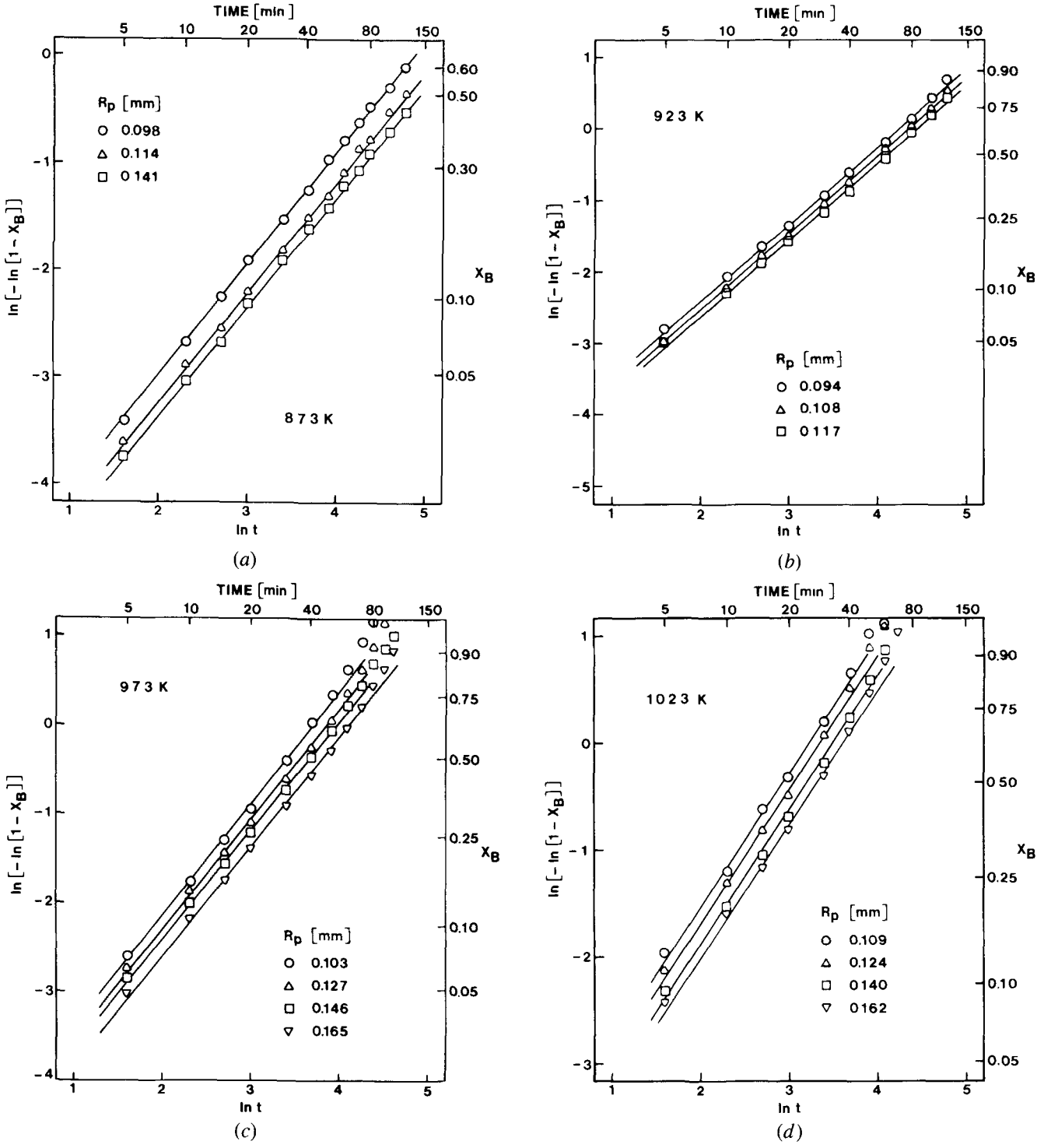

Fig. 10—Plot of $\ln[-\ln(1 - X_B)]$ *vs* $\ln t$ from the results of Figs. 5(a) through (d): (*a*) from the results of Fig 5(a), (*b*) from the results of Fig. 5(b), (*c*) from the results of Fig 5(c), and (*d*) from the results of Fig. 5(d).

growth product in the pellet at higher temperatures is somewhat different from the wire-shaped filaments formed at low temperatures as discussed earlier. Since the values of m are close to unity and it is convenient to use a constant value, $m = 1$ was used in determining the rate constant.

(2) From such a plot the value of S at each temperature was obtained from the intercept with the $\ln t = 0$ axis.

(3) On plotting S *vs* R_p^2 according to Eq. [8], the intercept with the $R_p^2 = 0$ axis provides the intrinsic value of the apparent rate constant k_b unaffected by diffusional effects, corresponding to a zero diffusion path length, at different temperatures as shown in Figure 11.

(4) The rate constant k was calculated using Eq. [4] since C_{H_2} is known at different temperatures. As noted earlier, it was determined that $f(C_{H_2}) = C_{H_2}$.

The intrinsic rate constants, obtained through the use of the procedure outlined above, are plotted against $1/T$ in Figure 12. The straight line through these data can be represented by

$$k = 4.08 \times 10^6 \exp\left(-\frac{E}{RT}\right) (\text{cm}^3 \cdot \text{mol}^{-1} \cdot \text{s}^{-1}) \qquad [10]$$

where $E = 92.0$ kJ/mol for the pellet-shaped samples.

The activation energies determined from both experiments using particles and pellets are identical, but the pre-exponential factors in Eqs. [6] and [10] are different by a factor of about two. The explanation may lie in the fact that the compaction (or pelletizing) increased the surface area of the solid. The specific surface area of the pellets is 1.26 times, on the average, that of the chalcocite before compaction, indicating some fracturing during compaction. Such fracturing is likely to be irregular and, therefore, may produce a compact with a wider distribution of grain size including finer particles. Furthermore, the formation of nuclei is greatly favored in general at sites where the lattice structure has been distorted by impurities, line defects, or mechanical deformation. Consequently, nuclei tend to form more readily on the grain boundaries, edges, and corners of the specimen than on the defect-free regions. These effects appear to have resulted in larger rates for the compacted samples.

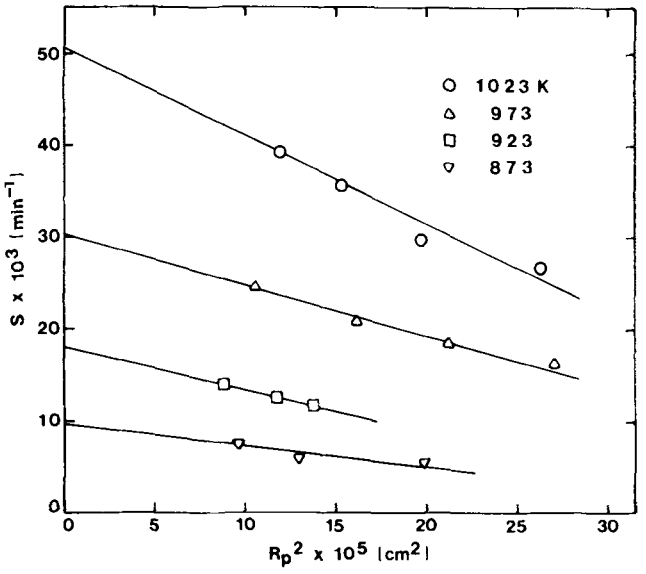

Fig. 11 — Plot of the extrapolation of kinetic data to zero pellet size in order to eliminate the effect of intrapellet diffusion ($p_{H_2} = 0.86$ atm).

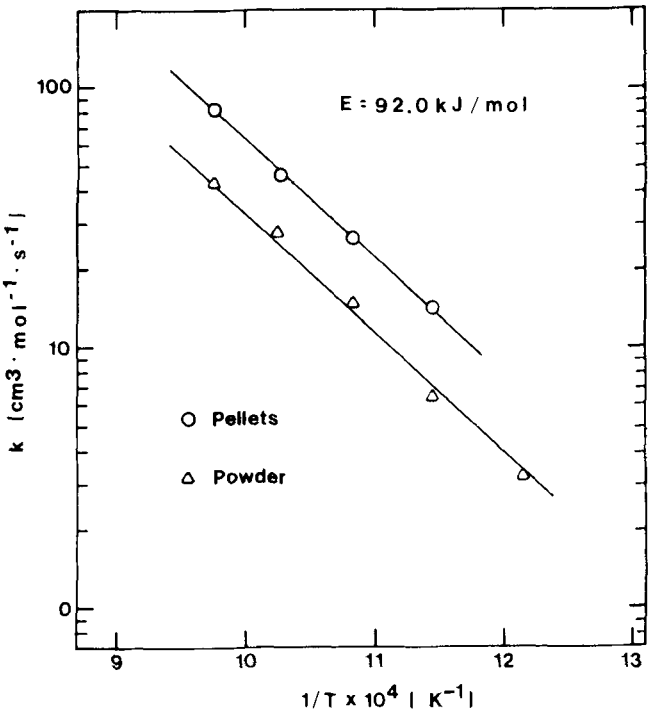

Fig. 12 — Arrhenius plot of rate constants for −325 +400 mesh Cu_2S particles obtained from loose particles and pellet experiments.

V. CONCLUSIONS

The hydrogen reduction of cuprous sulfide produced copper filaments in the temperature range 823 to 1023 K. The nucleation and growth kinetics expressed in Eq. [3] were found to be useful in describing the kinetics of the reaction. The activation energies determined from both the powder and the pellet experiments were found to be 92.0 kJ/mol, but the pre-exponential factor is higher (about two times) for porous pellets than for powder due to somewhat increased surface area during compaction. The reaction followed first-order kinetics with respect to the solid reactant as well as the hydrogen concentration. The rate of conversion for the hydrogen reduction of dense Cu_2S particles is thus given by

$$\frac{dX_B}{dt} = k_0 \cdot \exp(-11\,100/T) \cdot C_{H_2} \cdot (1 - X_B) \qquad [11]$$

with $k_0 = 2.23 \times 10^6$ for loose −325 +400 mesh particles. It has a somewhat larger value when the particles are compacted.

NOMENCLATURE

b	number of moles of solid reacted by one mole of gaseous reactant
C_{H_2}	molar concentration of hydrogen (mol · cm^{-3})
E	activation energy

k reaction-rate constant defined in Eq. [4] ($cm^3 \cdot mol^{-1} \cdot s^{-1}$)
k_b apparent rate constant given in Eqs. [3] and [4] (s^{-1})
k_0 pre-exponential factor for k ($cm^{-3} \cdot mol^{-1} \cdot s^{-1}$)
m constant in the nucleation and growth kinetics given in Eq. [3] (−)
R_p half thickness of the sample (cm)
S term defined by Eq. [7]
t time (s)
T temperature (K)
X_B fractional conversion of the solid (−)

ACKNOWLEDGMENTS

This work was supported in part by the State of Utah Mineral Leasing Fund, a grant from the University of Utah Research Committee, and a Camille and Henry Dreyfus Foundation Teacher-Scholar Award Grant to H. Y. Sohn. The authors acknowledge with thanks a Graduate Fellowship award to S. Won by the University of Utah Research Committee during this work, which was performed in partial fulfillment of the requirements for his Ph.D. degree.

REFERENCES

1. H Kay: *High-Temperature Refractory Metals*, W. A Krivsky, ed., Gordon and Breach, New York, NY, 1968, pp. 33-44
2. R. E. Cech and T. D. Tiemann: *TMS-AIME*, 1969, vol 245, pp 1727-33
3. F Habashi and R Dugdale: *Metall. Trans.*, 1973, vol. 4, pp. 1865-71
4. F. Habashi and B. I. Yostos· *J. Metals*, 1977, vol 29, no. 7, pp 11-16.
5 H Y. Sohn and K. Rajamani· *Chem. Eng. Sci.*, 1977, vol. 32, pp. 1093-101.
6. J. D. Spagnola: U S.B.M Rep. Invest., 6662, 1965.
7. T. Tanaka, H. Shimamura, and K. Jibiki· *Z. Phys. Chem.*, 1968, vol 61, pp. 113-42.
8 T Tanaka and H. Abe: *Erzmetall*, 1972, vol. 25, no. 4, pp. 181-87.
9. P C. Kapur, R. P Goel, G R K. Murty, and K. P. Singh· *J.I S.I*, 1972, vol. 210, pp. 698-701.
10 G. J. W. Kor: *Metall. Trans*, 1974, vol. 5, pp 339-43.
11. J. Mäkinen. "Kinetics and Morphology in the Reaction between Cuprous Sulphide and Hydrogen," Doctor Tech. Thesis, Helsinki University of Technology, Helsinki, 1975.
12. M. A. Fahim and J. D. Ford: *Can. J. Chem Eng*, 1976, vol. 54, pp. 578-83
13. T. Chida and J D. Ford: *Can. J. Chem Eng.*, 1977, vol. 55, pp 313-16.
14 R Hasegawa: *Trans. Nat. Res. Inst Metals (Japan)*, 1978, vol. 20, no. 2, pp. 111-27.
15. J. Szekely, C. I. Lin, and H. Y. Sohn. *Chem. Eng Sci.*, 1973, vol. 28, pp 1975-89.
16. J Szekely, J W. Evans, and H. Y. Sohn: *Gas-Solid Reactions*, Academic Press, New York, NY, 1976, pp. 231-40.
17. S. Won Ph D. Dissertation, Department of Metallurgy and Metallurgical Engineering, University of Utah, Salt Lake City, UT, 1982.
18 M Nagamori and T. R. Ingraham: *Metall. Trans.*, 1971, vol 2, pp 1501-03.
19 C Wagner *Trans. AIME*, 1952, vol. 194, pp. 214-16.
20 H K. Hardy: *Progress in Met. Phys*, 1956, vol. 6, pp. 45-73.
21. S. S. Brenner: *Acta Metall.*, 1956, vol. 4, pp. 62-74.
22 W A. Johnson and R F. Mehl: *TMS-AIME*, 1939, vol. 135, pp 416-58.
23 M Avrami. *J Chem. Phys.*, 1939, vol. 7, pp 1103-12.
24. P W. M. Jacobs and F. C Tompkins: in *Chemistry of the Solid State*, W E. Garner, ed., Butterworths, London, 1955, pp. 184-212.
25. D A Young. *The International Enclyclopedia of Physical Chemistry and Chemical Physics*, F C Tompkins, ed, Pergamon Press, Oxford, 1966, vol 1, topic 21.
26. H. Y Sohn: *Metall Trans. B*, 1978, vol. 9B, pp 89-96.
27. H. Y. Sohn and J Szekely· *Chem. Eng. Sci.*, 1972, vol. 27, pp 763-78.